

A Real-Time Model for Testing Stator-Ground Fault Protection Schemes of Synchronous Machines

A. B. Dehkordi, A. M. Gole, T. L. Maguire, P. Neti

Abstract—The paper presents a real time electromagnetic transient model for synchronous machines which is suitable for generating relay settings data for stator-ground fault protection schemes. Unlike conventional d-q based machine models the proposed model uses a winding function approach capable of representing non-sinusoidal windings and machine saturation accurately. This feature makes it possible for the model to accurately simulate the variation in the magnitude of third harmonic voltage in the neutral and terminals of synchronous machines. These harmonic signals are the basis of some stator-ground protection schemes. One of the requirements of such schemes is the evaluation of this harmonic voltage for different loading conditions, and correct representation of this signal is important for proper setting of the relay. In this paper, the third harmonic voltages of the neutral and terminal of a synchronous machine are evaluated using the developed real-time model. Laboratory results are provided to confirm the model operation.

Keywords: real-time simulation, synchronous machine, ground fault protection, saturation, cross-magnetization, winding function, Digital transient network analyzer.

I. BACKGROUND

Stator-ground faults are amongst the most frequent causes of the damage to the stator windings of synchronous machines and a direct cause of phase-phase faults [1]-[2]. A commonly used method for the detection of synchronous machines stator-ground faults is based on the existence of third harmonic voltage in the neutral and terminals of synchronous machines. These harmonic voltages are generated due to space harmonics of windings and non-sinusoidal permeance of the machine [3]. This scheme is generally used when the neutral of the machine is not solidly connected to ground, but is connected through impedance [4]. Fig. 1 is a conceptual circuit diagram of a synchronous machine supplying a Δ -connected load with the neutral connected to the ground through a resistance R_N . In Fig. 1, C_N represents the equivalent charging

capacitance of the stator winding to ground and C_T represents capacitance to ground seen from the stator terminal (windings, cables, etc.) [2]. When no fault is present, the voltages across the stator windings of the synchronous machine contain the fundamental component in addition to the odd harmonics [3]. As the machine is balanced, only the harmonics of order $3k, k \in 1, 3, \dots$ are present in the neutral-ground voltage of the machine v_N , whereas the terminal-ground voltage v_T contains the fundamental component and all the odd harmonics. The magnitude of the third harmonic voltage in the neutral and terminal of the machine, V_{N3} and V_{T3} during the normal operation depends on the magnitude of third harmonic voltage across the winding and impedance values of C_N, C_T and R_N [2]. During a stator-to-ground fault, the magnitude of the third harmonic component in the neutral, as well as on the phase terminals changes. This change is utilized as a signature to detect the ground fault [1],[2], [4].

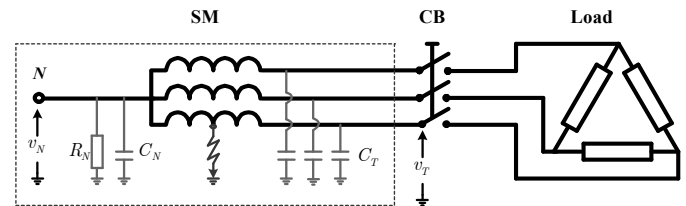


Fig. 1. Circuit diagram of the synchronous machine connected to a load.

As discussed above the third harmonic voltage exists even without a stator-ground fault and therefore in the industrial commissioning of such relays one of the requirements is recording these harmonic voltages at different operating points as the loading conditions affects the magnitude of these signals [2], [4]. At present, this procedure must be carried out individually for each machine type using a laboratory setup. In order to expedite the setting process, relay manufacturers and utilities have expressed the desire to have EMT-type models that would show this third harmonic behavior. Traditional d-q axis based models in EMT programs [5] are based on the assumption of sinusoidally distributed windings and permeance. Hence they cannot simulate the third harmonic in the unfaulted machine's neutral during healthy operation, as this time-harmonic arises from the space harmonics of the winding distribution.

This paper develops a detailed synchronous machine model which considers the actual distribution of the windings, shape of pole-arc and the effects of operating point dependent saturation [6],[7]. This ensures the correct modeling of harmonics such as the third harmonic voltage across the

Financial support for the research was provided by RTDS[®] Technologies Inc and the IRC program of the Natural Sciences and Engineering Research Council (NSERC) of Canada.

Ali Dehkordi is with the University of Manitoba, Winnipeg, Canada (e-mail: dehkordi@ee.umanitoba.ca).

Ani Gole is with the University of Manitoba, Winnipeg, Canada (e-mail: gole@ee.umanitoba.ca).

Trevor Maguire is with RTDS Technologies Inc., Winnipeg, Canada (e-mail: tlm@rtds.com).

Prabhakar Neti is with General Electric-Global Research Center, Niskayuna, NY 12309 USA (e-mail: netipr@ge.com).

Paper submitted to the International Conference on Power Systems Transients (IPST2009) in Kyoto, Japan June 3-6, 2009

winding and their variation with the loading. Furthermore, the model is developed for a real-time simulator (RTDS), so it can also be used for on-line closed-loop testing of relay performance.

II. DESCRIPTION OF THE SYNCHRONOUS MACHINE AND CAPABILITIES OF THE MODEL

The proposed machine model is applicable to any synchronous machine, but is intended for use with utility generators. However, for experimental validation, the authors did not have access to an actual utility generator, and hence a much smaller laboratory machine was used.

A. Experimental Machine

The machine under study is a 3kW, 4-pole, 60 Hz, 1800 rpm, 208 V (line-to-line), star connected salient-pole synchronous machine. The stator and a rotor lamination of this machine are shown in Fig. 2. The stator has a single layer, 3-phase, random-wound concentric winding distributed in 36 stator slots. Each phase of the stator winding has two series connected coils. There are 16 turns/slot/phase with a total of 96 turns per phase. The salient-pole rotor has 24 damper bars (6 bars/pole face). The turns-function [8] of stator phase-A is shown in Fig. 3. The turns-functions of phase-B and phase-C will be similar to that of the phase-A with phase shifts of $\pm 60^\circ$ mechanical ($\pm 120^\circ$ electrical).

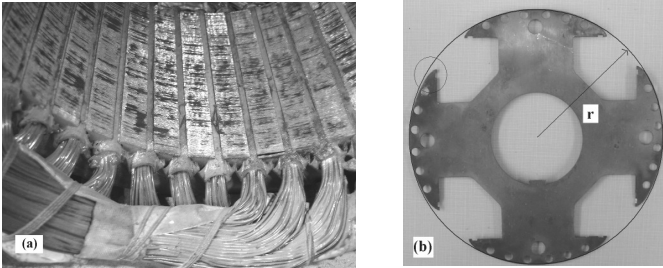


Fig. 2. Experimental synchronous machine: (a) stator, (b) rotor lamination

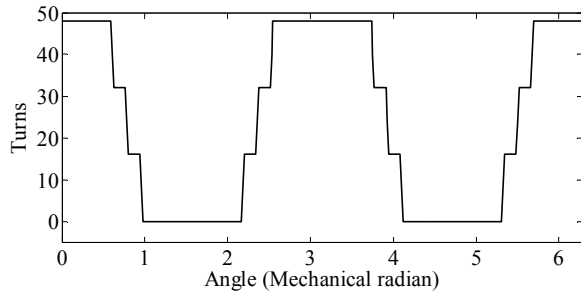


Fig. 3. The turns function of stator phase-A

The field winding consists of four coils connected in series with 500 turns in each coil. The turns-function of the rotor field winding is shown in Fig. 4.

The rotor pole-arc of the experimental machine is not exactly circular but has different curvatures along the pole-face [9]. The air-gap function of the machine is shown in Fig. 5, on which is also superposed a commonly used circular approximation where the air-gap is considered constant along the pole arc.

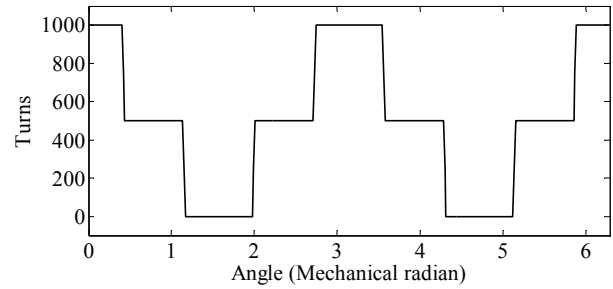


Fig. 4. The turns function of the field winding

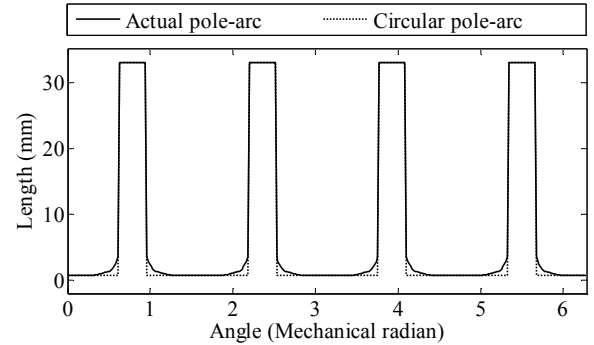


Fig. 5. The air-gap function considering actual rotor pole-arc

B. Inductance Calculation

For each rotor position, the inductances of the machine windings are computed using the modified winding function approach (MWFA) [8]. To account for additional effects (such as the stator and rotor slots and the non-circular rotor pole-arc) the permeance function is slightly modified into an ‘effective permeance function’ as proposed in [6],[7], using experimentally measured L_d , L_q and L_0 values. Fig. 6 shows the unsaturated self and mutual stator inductance values calculated using the MWFA and FEM. Two different values are shown for the MWFA; one (labeled Unmod) with the permeance function computed from the raw geometrical data and the other (labeled Effective) with the effective permeance function which, as evaluated by adjusting the unmodified permeance function using experimentally measured L_d , L_q and L_0 [6],[7],[10]. It can be seen that the stator inductances calculated using effective permeance function are very close to the result of FEM calculations, whereas the unmodified inductances have noticeable error. The actual curvatures of the pole-arc are considered in the calculation of the permeance function [7], therefore the harmonic content of the inductances are represented properly.

The effects of operating point dependent saturation are taken into account in the computation of inductances by adjusting the permeance function based on the magnitude and angle of total magneto-motive force [7], [11][12], therefore effects of cross-magnetization phenomenon are included in the model. The inductances of faulted windings can also be computed using the above procedure. Assume a situation where the stator phase-A is divided into two sub-windings A1 and A2; A1 has 80 turns and A2 contains the remaining 16. Fig. 7 shows the inductances of these faulted windings in a

loading condition where $i_{md} = 1.2$ pu and $i_{mq} = 1.4$ pu.

Values of the saturated inductances are stored as functions of d and q axis magnetizing currents (i_{md} and i_{mq}). In order to save on storage, rather than storing a table of inductance values versus the magnetizing currents for each angular position, only the dominant Fourier series magnitudes and phases are stored in tabular form. At any operating point (i_{md} and i_{mq} values). The actual inductance variation with angle can then quickly be formulated by evaluating the Fourier series at any angular position. Note that although the model is primarily not a d-q axis based model, d and q axis quantities are used to evaluate the saturated conditions only. Comparison with experiment validates this approach.

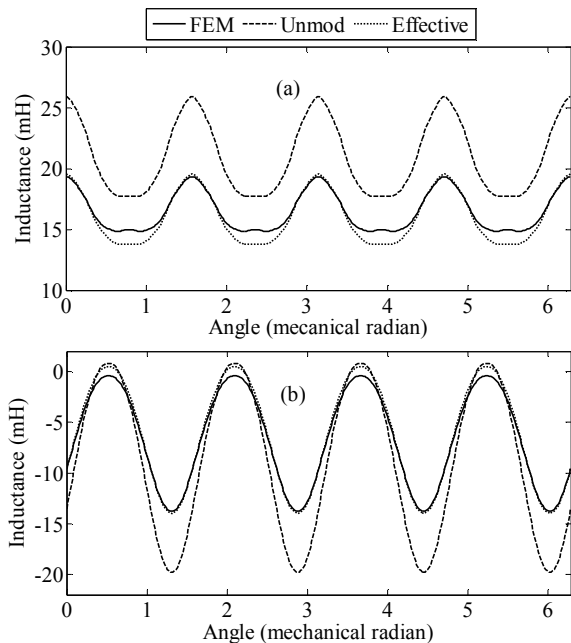


Fig. 6. Stator inductances using MWFA and FEM. (a) Self inductance of stator phase-A. (b) Mutual inductances between stator phase-A and phase-B

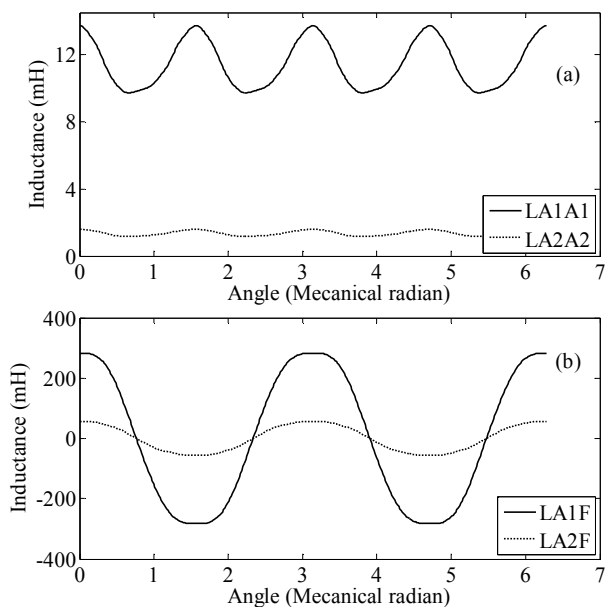


Fig. 7. Saturated inductances of faulted windings generated using MWFA a) Self inductance of windings A1 and A2, b) Mutual inductances between the field winding and sub-windings A1 and A2.

C. Time Domain Simulation in RTDS

There are two approaches for connecting a machine model to an EMTP type simulator. A commonly used approach is to use an *interfaced model* [5], which solves the machine equations independently and injects the resulting currents back into the main EMTP program. The advantage of this approach is that it is fast as it does not require repeated admittance matrix factorization each time for the new position of rotor. Alternatively, an *embedded model* makes the inductances of the machine part of the main network solution. As these inductances change with rotor position and saturation, the admittance matrix must be refactorized in each time step. This is time consuming, but on the other hand, the model is more accurate and less prone to numerical instability [13]. Therefore, in this paper the machine is modeled as a phase domain embedded model. In this approach the elements of the total admittance matrix which correspond to the machine nodes change their values in each time-step as rotor position and level of saturation changes. This improves the numerical stability of the model and a wide range of operating scenarios can be achieved.

III. EXPERIMENTAL VALIDATION

The embedded phase-domain machine model was incorporated into the real-time digital simulator (RTDS[®]). The model was thoroughly validated using laboratory experiments [7]. As the focus of this paper is the presence of third harmonic in the voltage across the windings, the experimental results presented in this paper validate the model regarding this matter.

Fig. 8a shows the simulated and experimentally obtained steady state phase-to-neutral voltage of the machine with a 0.95 pu resistive load (resistance of 15.2 Ω). The machine was operated as a generator in the steady state at the rated speed and 109 % of rated voltage. As can be seen the experimental and simulated results show a good agreement. Fig. 8b shows the harmonic content of the experimental and simulated voltages in Fig. 8a. The third harmonic component in the phase voltage is considerable (17.2 V). This value is 19.1 V in the simulated results.

In another test to show the performance of the model in highly saturated conditions, the machine is loaded with a leading power factor load which results in over voltage and hence drives the machine into saturation. In this scenario, the generator is running at rated speed and loaded with a Δ -connected R-C load (1.05 pu, at 0.5 pf). The field voltage is adjusted such that the open circuit voltage of the machine is 84% of rated voltage. Fig. 9a shows the simulated and experimentally obtained steady state phase-to-neutral voltage of the machine with this load. Again a good agreement can be observed for the simulated and experimentally obtained results. The harmonic spectrums of the voltages in this test are shown in Fig. 9b. The third harmonic components of the voltage here are 17.5 V and 18.0 V for experiment and simulation respectively.

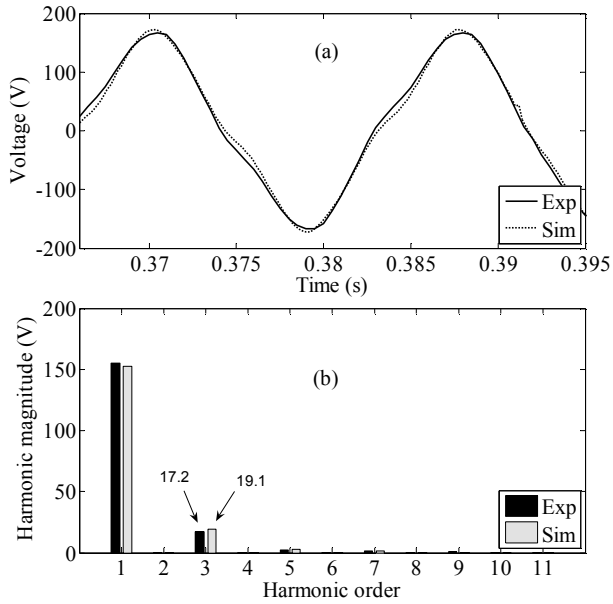


Fig. 8. Experimental and simulated voltage across the stator phase-A with a resistive load a) steady state waveform, b) harmonic spectrum (peak magnitude).

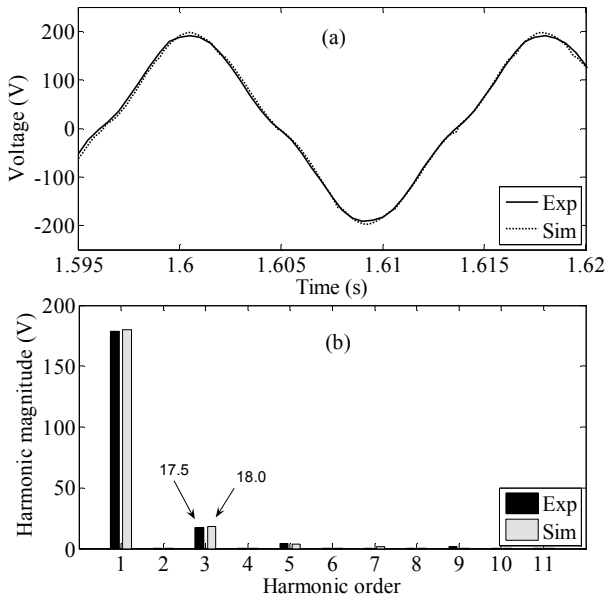


Fig. 9. Experimental and simulated voltage across the stator phase-A with R-C load a) steady state waveform, b) harmonic spectrum (peak magnitude).

IV. SIMULATIONS FOR THE PURPOSE OF RELAY SETTING DETERMINATION

In this Section, using the machine model presented in this paper the behaviour of the third harmonic voltage in the neutral and terminals of the machine is studied. This exercise demonstrates the capability of this real-time model in setting the relays designed to detect stator-ground faults in synchronous machine.

Fig. 10 shows the circuit as drawn in RSCAD, the Human-Machine interface for the RTDS simulator [14]. The machine is run at rated speed, and excitation voltage is set so that rated terminal voltage is achieved with a 1pu, 0.8 pf Δ -connected series R-L load. As can be seen the neutral and terminals are

connected to the ground using the neutral resistance and charging capacitances mentioned in Section I. the stator terminals are connected to a dynamic load which can be altered during the simulation in *RUN TIME* environment [14]. Node *NJA* demonstrates a point in the stator phase-A winding which divides phase-A into two sub-windings A1 and A2. In this example A1 has 80 turns and A2 contains the remaining 16. This node can be connected to ground through a fault model to simulate the effects of stator-ground fault. The circuit is simulated in *real-time* using on the *GPC card* of RTDS [14] with the simulation time-step of $50\mu s$.

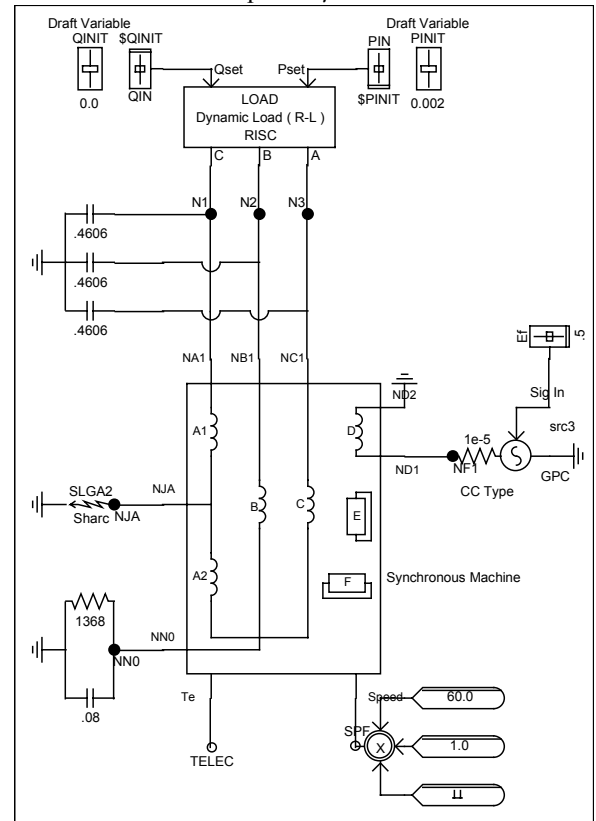


Fig. 10. RSCAD draft circuit used for the simulation.

Fig. 11a shows the variation of neutral voltage during a fault between node *NJA* and ground. As can be seen, before the fault this signal is mostly the third harmonic with the peak value of 13.1V. After the fault, the neutral voltage contains the fundamental harmonic as well, since the machine is operating in an unbalanced condition. The peak value of the third harmonic however is reduced to 2.1 V, as determined from Fourier analysis (not shown). The variation of neutral voltage during a fault between the terminal node *NA1* and the ground is shown in Fig. 11b, where the peak value of the third harmonic voltage changes from 13.1V to 15.8V. This SL-G fault is repeated with a dq-based machine and the results are shown in Fig. 11c. As can be seen, no voltage exists on the neutral of this machine before the fault, and this voltage contains only the fundamental frequency after the fault. This clearly shows that a conventional dq-based model would be inadequate for a real time simulator required for testing relays that protect against such faults.

As mentioned in Section I, in the industrial commissioning of relays designed to detect stator-ground faults, one of the requirements is recording the third harmonic voltage of terminal and neutral in different operating points. By running a pre-programmed automated sequence of runs, using the RSCAD's Script feature [14], the case in Fig. 10 is simulated in real-time on the RTDS hardware with the load absorbing various active and reactive powers. In each set of active and reactive powers the third harmonic component of the neutral and terminal voltages (V_{N3} and V_{T3}) are recorded after the circuit reaches the steady state condition.

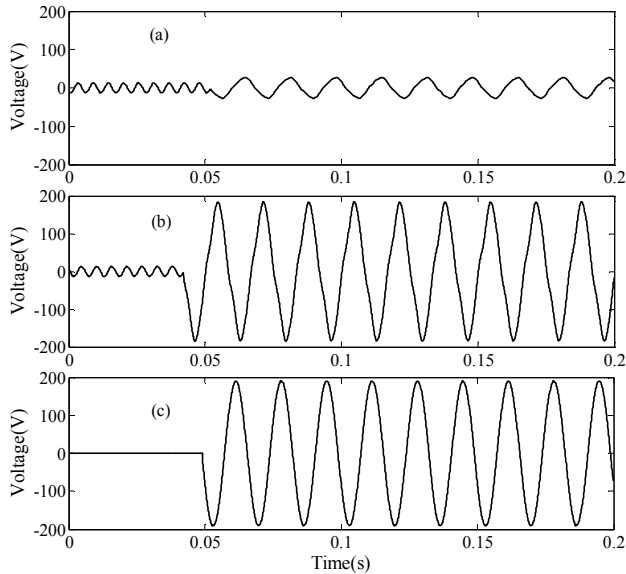


Fig. 11. Neutral voltage during a stator-ground fault a) ground fault on node NJA, b) ground fault on terminal node NAI, c) ground fault on terminal node NAI in a dq-based machine model.

Figures 12 and 13 show the variation of the third harmonic component in the neutral and the terminals respectively. These figures are generated by dynamically changing the resistor and inductances of the load and recording the active and reactive power of the load and the third harmonic component of the neutral and terminals voltages.

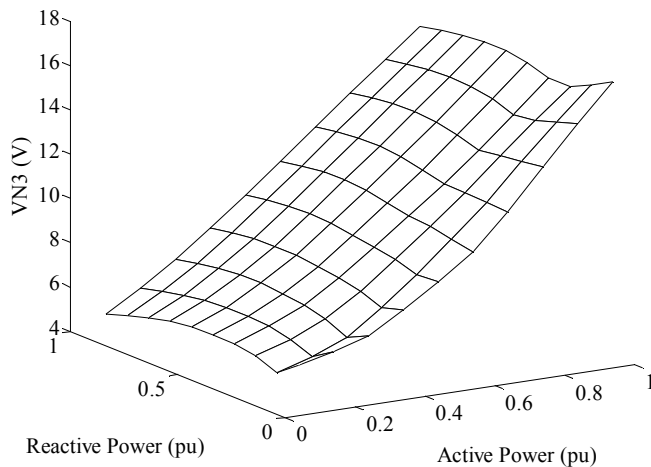


Fig. 12. Neutral voltage 3rd harmonic component as a function of active and reactive power loading

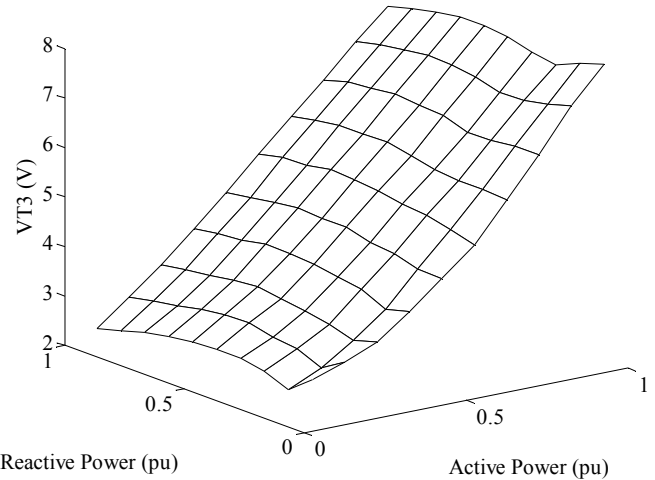


Fig. 13. Terminal voltage 3rd harmonic component as a function of active and reactive power loading

As can be seen the active power significantly affects the value of third harmonic voltage, which is also reported in [2]. The variation of the third harmonic voltage with the active power is comparable with the variation of this signal with a stator-to-ground fault. This confirms the need to record the pre-fault values of third harmonic voltage in the neutral and terminal to avoid ambiguity in detecting the fault. Using these pre-determined values for ambient 3rd harmonic voltage in stator and neutral terminals, the threshold settings for the relay can later be determined.

V. CONCLUSIONS

A detailed transient synchronous machine model was developed in this paper which is suitable for the use in testing relays for stator-ground fault detection. The model has the following important properties

- The machine inductances are computed using MWFA and effects of winding distribution and rotor geometry is considered in the calculation of inductances.
- The saturation is treated by adjusting the permeance of the machine based on local MMF magnitudes.
- A special feature of this model is the correct representation of time harmonics such as the third harmonic of the voltage. This was shown with the experimental validation.

It was demonstrated that this model can be used in setting the relays designed to detect the stator-ground faults in synchronous machines. Also closed-loop testing of such relays is possible as the model is implemented in the environment of the real-time digital simulator (RTDS[®]).

VI. APPENDIX

TABLE I

DQ0 PARAMETERS OF THE EXPERIMENTAL MACHINE

Parameter	Symbol	Value (p.u.)
D-axis inductance	L_d	0.81
Q-axis inductance	L_q	0.36
Zero sequence inductance	L_0	0.094
Stator resistance	R_s	0.043
Field resistance	R_f	0.011

TABLE II

MACHINE RATINGS AND GEOMETRICAL DATA

Machine Ratings	
Line-line rated voltage	208 V
Rated VA	3 kVA
Frequency	60 Hz
Number of phases	3
Field volts	120 V
Field amps	1.14 A
Number of poles	4
Stator Data	
Stator inner diameter	150 mm
Number of slots	36
Slots/phase/pole	3
Turns/coil	16
Number of layers	1
Number of series coils	2
Coil connection of phase A	1-12, 2-11, 3-10
Rotor Data	
Rotor outer diameter	148.6 mm
Stack length	90 mm
Pole-arc along d-axis	70.5 deg
Physical air-gap along d-axis	0.7 mm
Physical air-gap along q-axis	32.6 mm
Number of damper bars/pole	6
Field turns/coil	500

TABLE III

CIRCUIT PARAMETERS IN SIMULATION OF THIRD HARMONIC VOLTAGE IN THE NEUTRAL AND TERMINALS

Load inductance	L_L	68.9 mH
Load resistance	R_L	34.6 Ω
Field voltage	V_f	75.9 V
Neutral-ground charging capacitance	C_N	0.08 μ F
Neutral-ground resistance	R_N	1368 Ω
Terminal-ground charging capacitance	C_T	0.46 μ F

VII. ACKNOWLEDGMENT

The authors most gratefully and also sincerely appreciate the immense and high valued technical support from RTDS Technologies Inc. staff Dr. Khosro Kabiri, Dean Oullette and Heather Meiklejohn; and University of Manitoba technologist, Erwin Dirks.

VIII. REFERENCES

[1] C. H. Griffin and J. W. Pope, "Generator Ground Fault Protection Using Overcurrent, Overvoltage, and Undervoltage Relays," IEEE Transactions on Power Apparatus and Systems, vol. PAS-101, no. 12, pp. 4490–4497, Dec. 1982.

[2] M. Fulczyk, "Voltage 3rd harmonic in generator stator winding at changes in generator load conditions," IEEE International Electric Machines and Drives Conference, pp. 1476–1482, 2003.

[3] P. Neti, "Stator fault analysis of synchronous machines" Ph.D. Thesis, University of Victoria, 2007.

[4] *SEL-300G Generator Relay*, [Installation Manuel] Schweitzer Engineering Laboratories Inc., Pullman, WA, 2006.

[5] A.M. Gole, R.W. Menzies, D.A. Woodford and H. Turanli, "Improved interfacing of electrical machine models in electromagnetic transient programs," *IEEE Trans. Power Apparatus and Systems*, vol. PAS-103, no. 9, pp. 2446–2451, Sept. 1984.

[6] A. B. Dehkordi, P. Neti, A.M Gole, and T.L. Maguire, "Real-time simulation of internal faults in synchronous machines", *International Power System Transient Conference (IPST 2007)*, Lyon, June, 2007.

[7] A. B. Dehkordi, A.M Gole, and T.L. Maguire, "Development and Validation of a Comprehensive Synchronous Machine Model for a Real-Time Environment", *Accepted for Publication in IEEE Trans. Energy Conversion*, 2009.

[8] N.A. Al-Nuaim and H.A. Toliyat, "A novel method for modeling dynamic air-gap eccentricity in synchronous machines based on modified winding function theory," *IEEE Trans. On Energy Conversion*, vol. 13, no.2, pp. 156-162, June 1998.

[9] J.H.Walker, *Large synchronous machines - Design, Manufacture, and Operation*, Clarendon Press Oxford, 1981.

[10] P. Neti and S. Nandi, "Determination of effective air-gap length of synchronous reluctance motors (SynchRel) from experimental data", *IEEE-Transactions on Industry Applications*, Vol. 42, No.2, pp. 454-464, Mar. / Apr. 2006.

[11] E. Demeter, "Modeling of saturated cylindrical-rotor synchronous machines" Master's Thesis, University of Saskatchewan, July 1998.

[12] El-Serafi, A.M. and Kar, "Methods for determining the intermediate-axis saturation Characteristics of salient-pole synchronous Machines from the measured D-axis Characteristics", *IEEE Trans. On Energy Conversion*, vol. 20, no.1, pp. 88-97, Mar 2005.

[13] A.B. Dehkordi, A.M Gole, and T.L. Maguire, "Permanent magnet synchronous machine model for real-time simulation", *International Power System Transient Conference (IPST 2005)*, Montreal, June, 2005.

[14] *RTDS User's Manual*, RTDS Technologies Inc., Winnipeg, Canada, 2007.

IX. BIOGRAPHIES



A. B. Dehkordi (S'04) received the B.Sc. and M.Sc. degrees in electrical engineering from Sharif University of Technology, Tehran, Iran in 1999 and 2002 respectively. He worked as a research engineer for Sharif University of Technology in power quality projects in 2002. He is currently working towards his Ph.D. degree in the Department of Electrical and Computer Engineering at the University of Manitoba. His research is on the modeling of electric machines for the Real Time Digital Simulation. Mr. Dehkordi is a recipient of the MITACS Internship Scholarship Appointment through the NSERC Canada Network Centers of Excellence.



A. M. Gole (M'82, SM'04) obtained the B.Tech. (EE) degree from IIT Bombay, India in 1978 and the Ph.D. degree from the University of Manitoba, Canada in 1982. He is currently Senior NSERC Industrial Research Chair in Power Systems Simulation in at the University of Manitoba. Dr. Gole's research interests include the utility applications of power electronics and power systems transient simulation. As an original member of the design team, he has made important contributions to the PSCAD/EMTDC simulation program. Dr. Gole is the year 2007 recipient of the IEEE Power Engineering Society's Nari Hingorani FACTS Award.



T. L. Maguire (M'84, SM'04) was born in Canada. He graduated from the University of Manitoba with B.Sc.EE, M.Sc.EE and Ph.D. degrees in 1975, 1986, and 1992 respectively. Relevant employment experience includes time with Manitoba Hydro (1975-76), Manitoba HVDC Research Centre (1986-1994), and RTDS Technologies, Inc. (1994-present). He is a founding principal of RTDS Technologies, Inc. with a special interest in real-time simulation model development and also real-time simulation

digital hardware development. He participated in creating the world's first commercial real time digital power system simulator.



Prabhakar Neti (S'04, M'07) received the B.Tech. degree from Sri Venkateswara University, India, and the M.Tech. degree from Jawaharlal Nehru Technological University, India, in 1994 and 1996, respectively, both in electrical engineering. From 1996 to 2002, he served as a faculty member at different engineering colleges in India. He received the Ph.D. degree in electrical and computer engineering from the University of Victoria, Canada in 2007. From May 2007 to April 2008, he worked

as a Post Doctoral Fellow in the Department of Electrical and Computer Engineering, University of Manitoba, Canada. He is currently working at General Electric-Global Research Center, Niskayuna, NY, USA. His research interests are mainly in the area of modeling and fault diagnosis of electric machines and drives.